

Gadolinium Complexes of Bifunctional Diethylenetriaminepentaacetic Acid (DTPA)-bis(amides) as Copper Responsive Smart Magnetic Resonance Imaging Contrast Agents (MRI CAs)

Ki Soo Nam, Ji-Ae Park,[†] Ki-Hye Jung, Yongmin Chang,^{‡,§,*} and Tae-Jeong Kim^{*}

Department of Applied Chemistry, Kyungpook National University, Daegu 702-701, Korea. *E-mail: tjkim@knu.ac.kr

[†]Molecular Imaging Research Center, Korea Institute of Radiological and Medical Sciences, Seoul 139-706, Korea

[‡]Department of Medical & Biological Engineering, Kyungpook National University, Daegu 702-701, Korea

*E-mail: ychang@knu.ac.kr

[§]Department of Diagnostic Radiology & Molecular Medicine, Kyungpook National University, Daegu 702-701, Korea

Received June 10, 2013, Accepted July 4, 2013

We present the synthesis and characterization of DTPA-bis(histidylamide) (**1a**), DTPA-bis(aspartamide) (**1b**), and their gadolinium complexes of the type $[\text{Gd}(\text{L})(\text{H}_2\text{O})]$ (**2a**: L = **1a**; **2b**: L = **1b**). Thermodynamic stabilities and R_1 relaxivities of **2a-b** compare well with Omniscan[®], a well-known commercial, extracellular (ECF) MRI CA which adopts the DTPA-bis(amide) framework for the chelate: $R_1 = 5.5$ and 5.1 mM^{-1} for **2a** and **2b**, respectively. Addition of the Cu(II) ion to a solution containing **2b** triggers relaxivity enhancement to raise R_1 as high as 15.3 mM^{-1} , which corresponds to a 300% enhancement. Such an increase levels off at the concentration beyond two equiv. of Cu(II), suggesting the formation of a trimetallic (Gd/Cu₂) complex in situ. Such a relaxivity increase is almost negligible with Zn(II) and other endogenous ions such as Na(I), K(I), Mg(II), and Ca(II). *In vivo* MR images and the signal-to-noise ratio (SNR) obtained with an aqueous mixture of **2b** and Cu(II) ion in an 1:2 ratio demonstrate the potentiality of **2** as a copper responsive MRI CA.

Key Words : Gd-DTPA(bisamides), Histidine, Aspartic acid, Copper sensor, Smart MRI CA

Introduction

MRI is a powerful technique for noninvasive diagnosis of the human anatomy, physiology, and pathophysiology on the basis of superior spatial resolution and contrast useful in providing anatomical and functional images of the human body.¹ At the clinical level, MRI techniques are mostly performed employing Gd(III) chelates (GdL) to enhance the image contrast by increasing the water proton relaxation rate in the body.² Despite their wide and successful applications in clinics, however, conventional Gd(III)-based low-molecular weight CAs are mostly ECF agents exhibiting rapid extravasation from the vascular space. As a result, the time window for imaging is considerably reduced, thus limiting acquisition of high-resolution images.

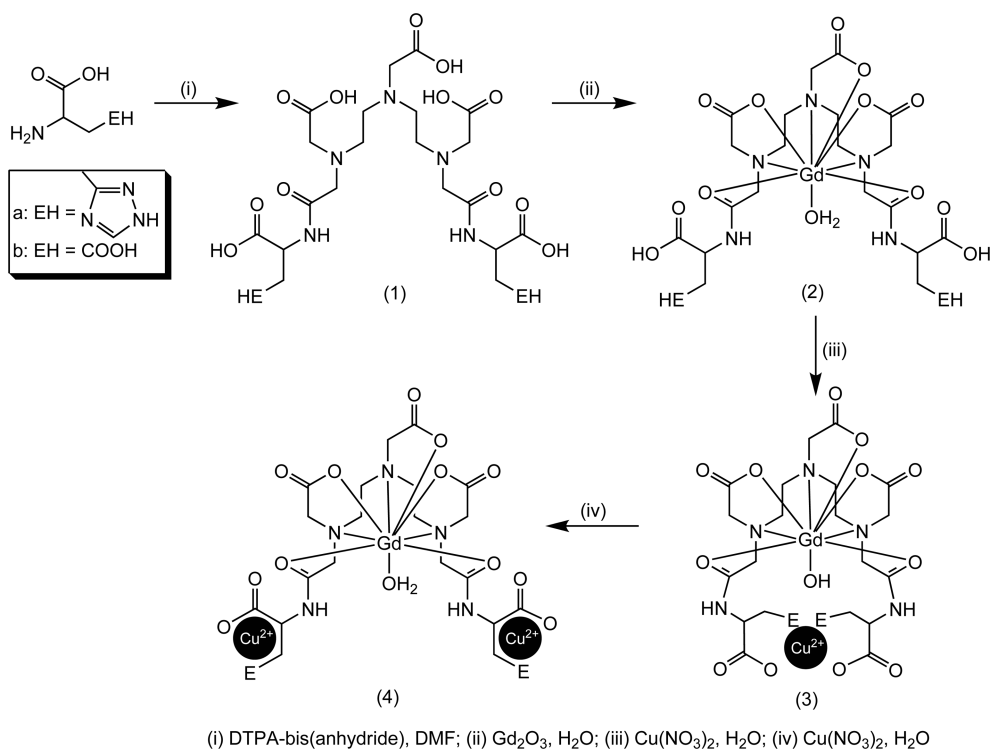
To overcome such limitations inherent to ECF MRI CAs, there has risen the necessity for the development of new MRI CAs carrying some unique functionality. In this regard, it is worth noting the recent advent of a variety of so-called 'targeting MRI CAs' capable of responding to particular organ(s),³⁻¹² pathologies (*i.e.*, tumors, angiogenesis, apoptosis),¹³⁻¹⁶ or biological stimuli (*i.e.*, pH,¹⁷ metal ions,¹⁸⁻²⁹ enzymes,³⁰⁻⁴⁰ glucose^{41,42}).

As part of our continued search for targeting MRI probes, we have recently reported a new bimodal magnetic resonance/single-photo emission computed tomography (MR/SPECT) imaging probe based on the multi-nucleating chelates (**1a-b**) such as shown in Scheme 1.⁴³ The observation that **1**

forms heterometallic Gd(^{99m}Tc) complexes has tempted us to prepare some new series of heterometallic complexes such as those incorporating both Gd and Cu for use as a potential Cu-sensitive MRI probe. Copper responsive MRI smart agents have recently been the subject of intense research activities due to the importance of copper in life.⁴⁴⁻⁵⁰ We now wish to report the synthesis of some new Gd complexes incorporated by bifunctional DTPA-bisamides and their evaluation as Cu-responsive smart MRI CAs.

Experimental

General. All reactions were performed under an atmosphere of dinitrogen using the standard Schlenk technique. Solvents were purified and dried using standard procedures. All reagents were purchased from commercial sources and used as received unless otherwise stated. Deionized water was used throughout all experiments. The ¹H NMR experiments were performed on a Bruker Advance 400 or 500 Spectrometer. Chemical shifts were given as δ values with reference to tetramethylsilane (TMS) as an internal standard. Coupling constants are in Hz. FAB-mass spectra were obtained by using a JMS-700 model (Jeol, Japan) mass spectrophotometer. Elemental analyses were conducted by using a Fisons EA 1108 model at Center for Instrumental Analysis, KNU. T_1 measurements were carried out using an inversion recovery method with a variable inversion time (TI) at 1.5 T (64 MHz). The magnetic resonance (MR) images were ac-



Scheme 1

quired at 35 different TI values ranging from 50 to 1750 ms. T_1 relaxation times were obtained from the non-linear least square fit of the signal intensity measured at each TI value. For T_2 measurements the CPMG (Carr–Purcell–Meiboom–Gill) pulse sequence was adapted for multiple spin-echo measurements. Thirty four images were acquired with 34 different echo time (TE) values ranging from 10 to 1900 ms. T_2 relaxation times were obtained from the non-linear least squares fit of the mean pixel values for the multiple spin-echo measurements at each echo time. Relaxivities (R_1 and R_2) were then calculated as an inverse of relaxation time per mM.

Potentiometric Measurements and Computational Method. Potentiometric titrations were performed with an automatic titrator to determine the protonation constants of the **1** and the stability constants of corresponding metal complexes (**2**). The autotitrating system consists of a 798 MPT titroprocessor, a 728 stirrer, and a PT-100 combination pH electrode (Metrohm). The pH electrode was calibrated using standard buffer solutions. All calibrations and titrations were carried out under a CO_2 -free nitrogen atmosphere in a sealed glass vessel (50 mL) thermostated at $25 \pm 0.1^\circ\text{C}$ at an ionic strength of 0.10 M KCl. The concentrations of the metal ion and the amide solutions were maintained at approximately 0.5 M. A CO_2 -free KOH solution (0.100 M) was used as a titrant to minimize the changes in ionic strength during the titration. Dioxygen and carbon dioxide were excluded from the reaction mixtures by maintaining a positive pressure of purified nitrogen in the titration cell. The electromotive force of the cell is given by $E = E' + Q \log [\text{H}^+] + E_j$, and both E' and Q were determined by titrating a

solution with a known hydrogen-ion concentration at the same ionic strength, using the acid range of the titration. The liquid-junction potential (E_j) was found to be negligible under the experimental conditions employed. The protonation constants of the ligands and the overall stability constants of various metal complexes formed in aqueous solutions were determined from the titration data using the computer program HYPERQUAD. The accuracy of this method was verified by measuring the protonation and the stability constants for $\text{Ca}(\text{II})$, $\text{Zn}(\text{II})$, $\text{Cu}(\text{II})$, and $\text{Gd}(\text{III})$ complexes of $[\text{DTPA-BMA}]^{3-}$. The results were compared with literature values.⁵¹

MR Imaging. MR images of anesthetized mice were obtained with a 1.5 T scanner (GE Sigma Advantage, GE Medical system, USA) and extremity coil. The mouse was placed in the magnet in a supine position with the heads firmly fixed. After each measurement the animal was revived from anesthesia, placed in the cage with free access to food and water. During the measurements, the animal was maintained at 37.0°C using a warm water blanket. The imaging parameters for FSPGR (fast spoiled gradient echo) are as follows: flip angle of 60° , 12×12 mm field of view, 256×128 matrix size, 22 axial slices, 2 mm slice thickness, slice gap of 0 mm, repetition time (TR) = 70 ms, echo time (TE) = 3 ms and number of acquisition (NEX) = 2.

In vivo Image Analysis. The anatomical locations with enhanced contrast were identified with respect to hepatocellular carcinoma of the liver on post-contrast MR images. For quantitative measurement, signal intensities in specific regions of interest (ROI) of $20\text{--}40\text{ mm}^3$ were measured using Advantage Window software (GE Medical, USA). Multiple

areas were sampled throughout the tumor and averaged to give a mean SI value for that tissue. The percentage of contrast enhancement in the signal from the tumor was calculated using the following equation, where SI is the signal to noise ratio: Enhancement (%) = 100 (SI_{post} - SI_{pre})/SI_{pre}.

Synthesis of 1a. To a suspension of histidine hydrochloride (1.5 g, 8.0 mmol) in CH₂Cl₂ (15 mL) was added triethylamine (5 mL). The mixture was stirred at room temperature for 1 h, after which DTPA-bis(anhydride) (1.4 g, 4.0 mmol) was in portions. The solution was further stirred for 6 h. The solvent was removed, and the residue taken up in methanol (5 mL) to be passed through a short silica gel column to remove any solid impurities. The solution was then applied to column chromatography with methanol as an eluent. The product was obtained as an off-white solid after removal of the solvent under vacuum. Yield: 0.87 g (81%). ¹H (DMSO-*d*₆) δ 8.47 (d, *J* = 7.52, 2 H), 7.75 (s, 2 H), 6.93 (s, 2 H), 4.50 (t, *J* = 6.52, 2 H), 3.46 (s, 2 H), 3.43 (s, 8 H), 3.29 (d, *J* = 6.52, 4 H), 2.87 (t, *J* = 5.02, 4 H), 2.85 (t, *J* = 5.02, 4 H). FABMS (*m/z*): Calc. for C₂₆H₃₈N₉O₁₂: 667.26 [M-H]⁺. Found: 668.27. Anal. Calc. for C₂₆H₃₇N₉O₁₂·H₂O: C, 45.55; H, 5.73; N, 18.39. Found: C, 45.64; H, 5.93; N, 18.33.

Synthesis of 1b. The title compound was synthesized in the same manner as described for the synthesis of **1a** by replacing histidine hydrochloride with L-aspartic acid (0.53 g, 4 mmol). The product was obtained as an off-white solid. Yield: 0.62 g (67%). ¹H (DMSO-*d*₆) δ 8.49 (d, *J* = 7.52, 2 H), 7.75 (s, 2 H), 6.93 (s, 2 H), 4.50 (t, *J* = 6.52, 2 H), 3.46 (s, 2 H), 3.43 (s, 8 H), 3.59 (d, *J* = 6.52, 4 H), 2.87 (t, *J* = 5.02 Hz, 4 H), 2.85 (t, *J* = 5.02, 4 H). FABMS (*m/z*): Calc. for C₂₂H₃₄N₅O₁₆: 624.20 [M-H]⁺. Found: 624.57. Anal. Calc. for C₂₂H₃₃N₅O₁₆: C, 42.30; H, 5.45; N, 11.22; Found: C, 42.45; H, 5.78; N, 11.16.

Synthesis of 2a. To a solution of **1a** (0.67 g, 1.0 mmol) in water (10 mL) was added Gd₂O₃ (0.18 g 0.5 mmol). The suspension was stirred for 6 h at 90 °C during which time a pale yellow solution resulted. The reaction mixture was cooled to RT and passed through a Celite to remove any solid impurities. The solvent was removed and the residue taken up in water (5 mL). Acetone (250 mL) was added to precipitate the product as a white solid. Yield: 0.56 g (78%). FABMS (*m/z*): Calcd for C₂₆H₃₅GdN₉O₁₂: 823.16 (M-H₂O)⁺. Found: 823.20. Anal. Calcd for C₂₆H₃₅GdN₉O₁₂·2.5H₂O: C, 35.29; H, 4.67; N, 14.25. Found: C, 35.39; H, 4.42; N, 13.84.

Synthesis of 2b. The title compound was synthesized in the same manner as described for the synthesis of **2a** by replacing **1a** with **1b**. Yield: 0.65 g (84%). FABMS (*m/z*): Calcd for C₂₂H₃₁GdN₅O₁₆: 779.10 (M-H₂O)⁺. Found: 779.15. Anal. Calcd for C₂₂H₃₁GdN₅O₁₆·3H₂O: C, 31.09; H, 4.51; N, 8.24. Found: C, 31.50; H, 4.46; N, 8.24.

Results and Discussion

Synthesis. Our design strategy for a copper-selective MRI CA relies on utilizing the bisamide side-arms of DTPA for bimetallic coordination leading to the formation of hetero-

trinuclear complexes in situ. The synthetic route to **3** and **4** and their proposed action for sensing Cu²⁺ are shown in Scheme 1. The reactions of DTPA-bis(anhydride) with aspartic acid and histidine provide in good yields the corresponding DTPA-bis(amide) conjugates **1a** and **1b**, respectively. Their subsequent reactions with Gd₂O₃ led to the formation of **2a** and **2b** as hygroscopic white solids. All new compounds were identified by microanalysis and spectroscopic techniques such as ¹H NMR and mass spectrometry.

Protonation and Stability Constants. The protonation constants of the bifunctional chelates (L = **1a-b**), $K_i^H = [H_iL]/[H_{i-1}L][H^+]$, were determined by potentiometric titration. The calculated protonation constants for the chelates are presented in Table 1 along with those for parent DTPA and DTPA-BMA for comparative purposes. In the case of DTPA-based ligands, the first protonation takes place at the central nitrogen atom, while the second and the third at the terminal amine nitrogen atoms. Quite expectedly, both **1a** and **1b** exhibit higher first protonation constants (log K_1^H) than DTPA-BMA. These observations suggest that the presence of carboxylic acid in the amide side-arm renders the protonation of the central amine nitrogen facile through a certain cooperative interaction, possibly through hydrogen bonding between the COOH group in the amide side-arm and the acetate arm on the central amine nitrogen. Yet, such a cooperative interaction seems to be less conspicuous in the case of **1b** lacking the COOH group in the amide side-arm.

Also listed in Table 1 are the thermodynamic stability constants (K_{GdL}) and selectivity constants (K'_{sel}) of corresponding gadolinium complexes (GdL = **2a-b**) and of other endogenous ions such as Ca(II), Zn(II), and Cu(II). The

Table 1. Protonation, stability, and selectivity constants for ligands and metal complexes

Equilibrium	logK (25 °C, μ = 0.10 M (KCl))			
	L = 1a	L = 1b	L = DTPABMA ^a	L = DTPA ^b
[HL]/[L][H]	9.52	11.55	9.37	10.49
[H ₂ L]/[HL][H]	7.59	9.42	4.38	8.60
[H ₃ L]/[H ₂ L][H]	6.52	5.92	3.31	4.28
[H ₄ L]/[H ₃ L][H]	3.82	2.04	-	2.64
ΣpK _a	27.45	28.93	17.06	26.01
[GdL]/[Gd][L]	19.59	21.12	16.85	22.46
logK _{GdL} ^c	17.03	14.93	14.84	18.14
[CaL]/[Ca][L]	6.96	10.18	7.17	10.75
logK _{CaL} ^c	4.30	4.01	5.11	6.43
[ZnL]/[Zn][L]	10.93	14.67	12.04	18.70
logK _{ZnL} ^c	8.37	8.48	10.02	14.38
[CuL]/[Cu][L]	10.98	14.78	13.03	21.38
logK _{CuL} ^c	8.42	8.59	11.06	17.06
logK _{sel} ([Gd]/[Ca])	12.73	10.92	9.68	11.71
logK _{sel} ([Gd]/[Zn])	8.66	6.45	4.81	3.76
logK _{sel} ([Gd]/[Cu])	8.66	6.34	3.82	1.08
logK' _{sel}	19.59	10.74	9.03	7.04

^{a,b}Data obtained from ref.⁵¹ ^cMeasured at pH 7.4.

Table 2. The pM values of metal complexes^a

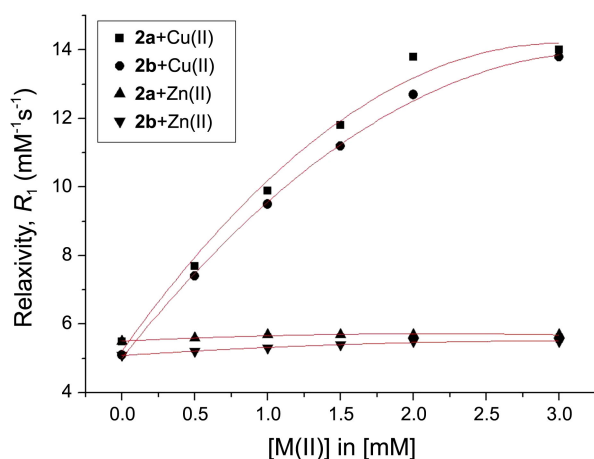
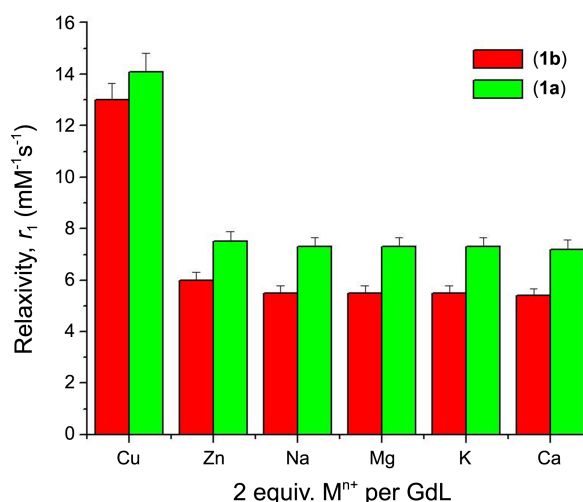
Equilibrium	logK (25 °C, $\mu = 0.10$ M (KCl))			
	L = 1a	L = 1b	L = DTPABMA ^b	L = DTPA ^c
pGd	16.03	13.93	13.88	17.14
pCa	3.30	3.01	4.19	5.45
pZn	7.37	7.48	9.06	13.39
pCu	7.42	7.59	10.05	16.06

^apM = $-\log[M^{n+}]_{\text{free}}$ at pH 7.4; $[M^{n+}]_{\text{total}} = 1 \mu\text{M}$; $[L]_{\text{total}} = 1.1 \mu\text{M}$. ^{b,c}Data obtained from ref.⁵¹.

direct potentiometric titration method cannot be applied to the measurement of the stability constants of Gd complexes of bisamides since they are formed at low pH. Instead, they were determined by employing the method of ligand-ligand competition potentiometric titration between EDTA and bisamides for Gd(III). The most characteristic feature of Table 1 is that gadolinium of all metals forms the most stable complexes regardless of the type of the chelate. When the comparison is made between Gd complexes of histidine (**1a**) and of aspartic acid (**1b**), the latter forms a more stable complex for the reason unknown.

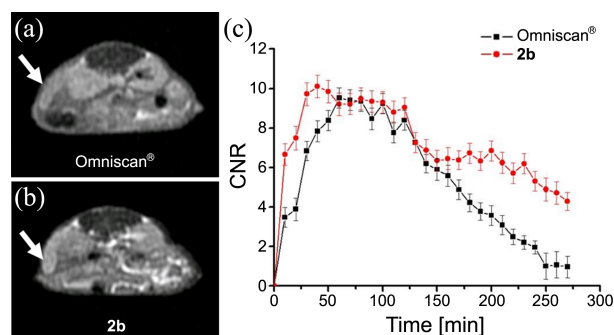
Table 2 lists the pM values for various metal ions. The thermodynamic stability constant alone is insufficient to account for the stability of the complexes under the physiological condition.^{17,18} Therefore, the conditional stability constant or more frequently the pM value is apt to describe the stability of complexes under physiologically relevant conditions.¹⁹ The pM value reflects the influence of ligand basicity and protonation of the complex.²⁰ Thus, the larger the pM value, the higher the affinity of the ligand for the metal ion under the given conditions. Table 2 shows that higher pM values are achieved with Gd(III) than with Ca(II), Zn(II), or Cu(II): Indication is that complexes **2a-b** are stable enough to avoid any interference by other endogenous metal ions.

Relaxivity. The ability of Cu(II) to modulate the longitudinal relaxivity of **2** was determined at 25 °C using T_1 measurements at 1.5 T. Spectroscopic measurements were

**Figure 1.** Plots of R_1 relaxivities of **2a** and **2b** as functions of $[M^{2+}]$ ($M = \text{Cu}, \text{Zn}$).**Figure 2.** Relaxivity response of **2a** and **2b** to various metal ions.

carried out under simulated physiological conditions (PBS, pH 7.4). Compounds **2a-b** show high stability in PBS for as long as a few days. In the absence of Cu(II), the R_1 relaxivities of **2a** and **2b** are 5.5 and 5.1 mM^{-1} , respectively. The addition of Cu(II) triggers signal enhancement, and R_1 gradually increases to reach the maximum value of 15.3 mM^{-1} until it eventually levels off at the concentration beyond two equiv. of Cu(II). These observations may be rationalized in terms of a pair of amide side-arms involved in coordination with two equivalents of Cu(II) ion to form in situ heterobimetallic (GdCu) and heterotrimetallic (GdCu_2) complexes (Scheme 1). Such a coordinative interaction is negligible in the case of Zn(II) as we observe virtually no changes in R_1 (Figure 1). The same is true with other endogenous ions such as Na(I), K(I), Mg(II), and Ca(II) as observed from Figure 2. The figure demonstrates high and unique sensitivity of **2** toward Cu(II) as compared with other metal ions. The mechanism for such a high relaxivity response of **2** toward Cu(II) has yet to be further investigated and the subject of future studies.

In vivo MR Imaging. Figures 3(a)-(b) show the T_1 -weighted images of mice bearing hepatocellular carcinoma (HCC) after the injection of $[\text{Gd}(\text{DTPA-BMA})(\text{H}_2\text{O})]$ (Omniscan[®])

**Figure 3.** The T_1 -weighted images of the tumor bearing H-ras transgenic mice with (a) Omniscan[®] and (b) **2b** saturated with 2 equiv. Cu(II). (c) Contrast-to-noise ratio (CNR) as a function of time measured with Omniscan[®] (square) and **2b** saturated with 2 equiv. Cu(II) (circle) at the dosage of 1 mmol/kg.

and the in situ trimetallic solution (**2b**/2 [Cu²⁺]), respectively. Most notably, the latter solution exhibits higher contrast enhancement than Omniscan®. The contrast-to-noise ratio (CNR) profiles shown in Figure 3(c) are consistent with these observations in that with this trimetallic system, the initial MR signal intensity is higher and the excretion rate lower than with Omniscan®.

Conclusions

We have put a new entry into a copper responsive MRI smart agent derivable from the Gd complexes (**2a-b**) of bifunctional DTPA-bis(amides), where the bifunctional chelates are DTPA-bis(histidylamide) (**1a**) and DTPA-bis(aspartamide) (**1b**). Complexes **2** show thermodynamic stabilities and *R*₁ relaxivities comparable with those of Omniscan®. Addition of the Cu(II) ion to a solution containing **2b** triggers a 300% relaxivity enhancement, and such an increase levels off at the concentration beyond two equiv. of Cu(II), suggesting the formation of a trimetallic (Gd/Cu₂) complex in situ. The observations that such relaxivity increases are almost negligible with other endogenous M(II) ions (M = Na, K, Mg, Ca, Zn), along with the observation that *in vivo* MR images and the CNR profiles obtained with **2b** saturated with 2 equiv. of Cu(II) demonstrate the potentiality of **2** as a copper responsive MRI CA.

Acknowledgments. T.-J.K. gratefully acknowledges the NRF for financial support (Grant No. 2012-0006388). NMR and mass spectral measurements were performed by KBSI.

References

- Caravan, P. *Chem. Soc. Rev.* **2006**, 35, 512.
- Caravan, P.; Ellison, J. J.; McMurry, T. J.; Lauffer, R. B. *Chem. Rev.* **1999**, 99, 2293.
- Aime, S.; Dastru, W.; Crich, S. G.; Gianolio, E.; Mainero, V. *Biopolym.* **2002**, 66, 419.
- Caravan, P. *Acc. Chem. Res.* **2009**, 42, 851.
- Caravan, P.; Zhang, Z. *Eur. J. Inorg. Chem.* **2012**, 2012, 1916.
- Geraldes, C. F.; Laurent, S. *Contrast Media Mol. Imaging* **2009**, 4, 1.
- Henrotte, V.; Vander Elst, L.; Laurent, S.; Muller, R. N. *J. Biol. Inorg. Chem.* **2007**, 12, 929.
- Jacques, V.; Desreux, J. F. *Top. Curr. Chem.* **2002**, 221, 123.
- Lattuada, L.; Barge, A.; Cravotto, G.; Giovanzana, G. B.; Tei, L. *Chem. Soc. Rev.* **2011**, 40, 3019.
- Clark, R. B. *Top. Curr. Chem.* **2002**, 221.
- Schmitt-Willich, H.; Brehm, M.; Ewers, C. L. J.; Michl, G.; Muller-Fahnow, A.; Petrov, O.; Platzek, J.; Raduchel, B.; Sulzle, D. *Inorg. Chem.* **1999**, 38.
- Uggeri, F.; Aime, S.; Botta, P. L. A. M.; Brocchetta, J. M.; Ermondi, C. d. H. G.; Grandi, M.; Paolio, P. *Inorg. Chem.* **1995**.
- Aime, S.; Botta, M.; Garino, E.; Crich, S. G.; Giovanzana, G.; Pagliarin, R.; Palmisano, G.; Sisti, M. *Chem.-Eur. J.* **2000**, 6, 2609.
- Chong, H. S.; Song, H. A.; Ma, X.; Lim, S.; Sun, X.; Mhaske, S. B. *Chem. Commun.* **2009**, 3011.
- Barrio, J. R.; Satyamurthy, N.; Huang, S.-C.; Petri, A.; Small, G. W.; Kepe, V. *Acc. Chem. Res.* **2009**, 42, 842.
- Tweedle, M. F. *Acc. Chem. Res.* **2009**, 42, 958.
- Giovanzana, G. B.; Negri, R.; Rolla, G. A.; Tei, L. *Eur. J. Inorg. Chem.* **2012**, 2012, 2035.
- Angelovski, G.; Fouskova, P.; Mamedov, I.; Canals, S.; Toth, E.; Logothetis, N. K. *Chembiochem.* **2008**, 9, 1729.
- Mishra, A.; Fousková, P.; Angelovski, G.; Balogh, E.; Mishra, A. K.; Logothetis, N. K.; Tóth, É. *Inorg. Chem.* **2008**, 47, 1370.
- Dhingra, K.; Fouskova, P.; Angelovski, G.; Maier, M. E.; Logothetis, N. K.; Toth, E. *J. Biol. Inorg. Chem.* **2008**, 13, 35.
- Dhingra, K.; Maier, M. E.; Beyerlein, M.; Angelovski, G.; Logothetis, N. K. *Chem. Commun.* **2008**, 3444.
- Hanaoka, K.; Kikuchi, K.; Urano, Y.; Nagano, T. *J. Chem. Soc. Perkin Trans. 2* **2001**, 1840.
- Major, J. L.; Parigi, G.; Luchinat, C.; Meade, T. J. *Proc. Natl. Acad. Sci. U. S. A.* **2007**, 104, 13881.
- Major, J. L.; Boiteau, R. M.; Meade, T. J. *Inorg. Chem.* **2008**, 47, 10788.
- Hanaoka, K.; Kikuchi, K.; Urano, Y.; Narazaki, M.; Yokawa, T.; Sakamoto, S.; Yamaguchi, K.; Nagano, T. *Chem. Biol.* **2002**, 9, 1027.
- Trokowski, R.; Ren, J.; Kalman, F. K.; Sherry, A. D. *Angew. Chem., Int. Ed.* **2005**, 44, 6920.
- Li, W.-h.; Parigi, G.; Fragai, M.; Luchinat, C.; Meade, T. J. *Inorg. Chem.* **2002**, 41, 4018.
- Li, W.-h.; Fraser, S. E.; Meade, T. J. *J. Am. Chem. Soc.* **1999**, 121, 1413.
- Zhang, X.-a.; Lovejoy, K. S.; Jasanoff, A.; Lippard, S. J. *Proc. Natl. Acad. Sci. USA.* **2007**, 104, 10780.
- Nivorozhkin, A. L.; Kolodziej, A. F.; Caravan, P.; Greenfield, M. T.; Lauffer, R. B.; McMurry, T. J. *Angew. Chem., Int. Ed.* **2001**, 40, 2903.
- Zhao, M.; Josephson, L.; Tang, Y.; Weissleder, R. *Angew. Chem., Int. Ed.* **2003**, 42, 1375.
- Moats, R. A.; Fraser, S. E.; Meade, T. J. *Angew. Chem., Int. Ed.* **1997**, 36, 725.
- Duimstra, J. A.; Femia, F. J.; Meade, T. J. *J. Am. Chem. Soc.* **2005**, 127, 12847.
- Yoo, B.; Pagel, M. D. *J. Am. Chem. Soc.* **2006**, 128, 14032.
- Mizukami, S.; Takikawa, R.; Sugihara, F.; Hori, Y.; Tochio, H.; Ichli, M. W.; Shirakawa, M.; Kikuchi, K. *J. Am. Chem. Soc.* **2008**, 130, 794.
- Louie, A. Y.; Hüber, M. M.; Ahrens, E. T.; Rothbächer, U.; Moats, R.; Jacobs, R. E.; Fraser, S. E.; Meade, T. J. *Nature Biotech.* **2000**, 18, 321.
- Querol, M.; Chen, J. W.; Weissleder, R.; Alexei Bogdanov, J. *Org. Lett.* **2005**, 7, 1719.
- Chauvin, T.; Durand, P.; Bernier, M.; Meudal, H.; Doan, B. T.; Noury, F.; Badet, B.; Beloeil, J. C.; Toth, E. *Angew. Chem. Int. Ed.* **2008**, 47, 4370.
- Giardiello, M.; Lowe, M. P.; Botta, M. *Chem. Commun.* **2007**, 4044.
- Hanaoka, K.; Kikuchi, K.; Terai, T.; Komatsu, T.; Nagano, T. *Chem.-Eur. J.* **2008**, 14, 987.
- Zhang, S.; Trokowski, R.; Sherry, A. D. *J. Am. Chem. Soc.* **2003**, 125, 15288.
- Trokowski, R.; Zhang, S.; Sherry, A. D. *Bioconjug Chem.* **2004**, 15, 1431.
- Park, J.-A.; Kim, J. Y.; Kim, H.-K.; Lee, W.; Lim, S. M.; Chang, Y.; Kim, T.-J.; Kim, K. M. *ACS Med. Chem. Lett.* **2012**, 3, 299.
- Jung, K. H.; Kim, H. K.; Lee, G. H.; Kang, D. S.; Park, J. A.; Kim, K. M.; Chang, Y. M.; Kim, T. J. *J. Med. Chem.* **2011**, 54, 5385.
- Que, E. L.; Chang, C. J. *Chem. Soc. Rev.* **2010**, 39, 51.
- Que, E. L.; Domaille, D. W.; Chang, C. J. *Chem. Rev.* **2008**, 108, 1517.
- Que, E. L.; Gianolio, E.; Baker, S. L.; Aime, S.; Chang, C. J. *Dalton Trans.* **2010**, 39, 469.
- Que, E. L.; Gianolio, E.; Baker, S. L.; Wong, A. P.; Aime, S.; Chang, C. J. *J. Am. Chem. Soc.* **2009**, 131, 8527.
- Viguier, R. F. H.; Hulme, A. N. *J. Am. Chem. Soc.* **2006**, 128, 11370.
- Zeng, L.; Miller, E. W.; Pralle, A.; Isacoff, E. Y.; Chang, C. J. *J. Am. Chem. Soc.* **2006**, 128, 10.
- Gu, S.; Kim, H. K.; Lee, G. H.; Kang, B. S.; Chang, Y.; Kim, T. J. *J. Med. Chem.* **2011**, 54, 143.